NUMERICAL SIMULATION OF THE INTERACTION BETWEEN THE JET AND A PELTON RUNNER UNDER LOW HEAD

Jean, Decaix[1], Anthony, Gaspoz
Institute of Sustainable Energy, School of Engineering, HES-SO Valais-Wallis, Switzerland
jean.decaix@hevs.ch, anthony.gaspoz@hevs.ch

Steve, Crettenand
Forces Motrices Valaisannes, Sion, Switzerland
Steve.Crettenand@fmv.ch

Cécile, Münch-Alligné,
Institute of Sustainable Energy, School of Engineering, HES-SO Valais-Wallis, Switzerland
Institute of Systems Engineering, School of Engineering, HES-SO Valais-Wallis, Switzerland
cecile.muench@hevs.ch

KEY WORDS

Pelton, CFD, Two-Phase Flow, URANS

ABSTRACT

In Switzerland, during the last decade, the development of the new renewable energies (small hydro, solar, wind…) has been promoted by a specific feed-in tariff. However, the regulator schedules to remove this specific measure to force the producers to match the demand. Regarding the small hydropower plants, this change requires to increase the flexibility of the power plants.
The present work focuses on the hydro power plant of Gletsch-Oberwald (KWGO, Valais, Switzerland), a run-of-river power plant equipped with two six-jet Pelton turbines. An extension of the flexibility of the power plant is investigated in the framework of the SmallFlex project by using one-third of the headrace tunnel as a storage volume. The use of this new storage capacity would require emptying the headrace tunnel and to operate the Pelton turbines at a lower head than the one for which they have been designed. By lowering the head, the efficiency of the Pelton turbines will decrease abruptly if the Pelton turbines make faces to the so-called "falaise" effect. Before performing on-site measurements, unsteady two-phase flow simulations of the interaction between the jet and the Pelton runner have been carried out for four different heads with the Ansys CFX software. At the best efficiency point, the efficiency is well predicted by the simulation. For lower heads, the interaction between two consecutive jets is observed but the decrease in efficiency is underestimated compared to the on-site measurements.

1. INTRODUCTION

The part of new renewable energies (solar, wind, biogas and biomass) in the energy production in Switzerland increased by 60% between 2015 [1] and 2019 [2] accounting for 4.2% of the electricity production. These sources of energy are characterized by their intermittency that can cause power network instabilities [3]. Moreover, Switzerland changed its national feed-in tariff (FIT) system in 2017 for small hydropower (representing 5% of the electricity production [4]) to encourage plant owners to produce according to the energy demand [5]. Consequently, the power plant production must be more and more flexible.
In this context, the SmallFlex project has be defined to investigate the possibility of increasing the flexibility of a run of river power plant equipped with Pelton turbines [6]. Among the tasks achieved during the project, one focuses on the use of the upper part of the headrace tunnel as an additional storage volume. However, using this volume requires to operate the Pelton turbine to a lower head that initially scheduled. The efficiency of a Pelton turbine is strongly influenced by the head available since for a specific threshold, the efficiency drops abruptly with an increase in mechanical stresses and fatigue [7]. This phenomenon is called "falaise"

[1] Corresponding author

effect [8] and is discussed in some books such as [9]. However, this phenomenon does not seem to have been studied either experimentally nor numerically, even if numerical simulations of Pelton turbines have been already performed to investigate the efficiency of a two-jet Pelton turbine [10], to develop a new Pelton turbine [11], to understand the risk of bucket cavitation ([12],[13]) or the influence of the jet quality on the turbine efficiency ([14],[15]). Furthermore, in the last decade several mesh free solvers have been developed to investigate the interaction between the jet, the buckets and the Pelton casing or the risk of erosion ([16],[17],[18]). However, following the review by Židonis [19], the finite volume software Ansys CFX is the one that provides the best accuracy.
Consequently, this paper aims at investigating the occurrence of the "falaise" effect by CFD. It is organized as follows: the test case is first described, followed by the description of the numerical set up, then the results are discussed and compared with on-site measurements and finally a conclusion is written.

2. TEST CASE

The power plant of Gletsch-Oberwald (KWGO), owned by FMV, is a small run-of-river power plant equipped with two six-jet Pelton turbines. The Pelton turbine is characterized by a rotational speed of 600 rpm and a nominal power of 7 MW for a nominal head of 287 m and a nominal discharge of 2.81 m^3/s. The Pelton wheel has 21 buckets (see Figure 1).
The additional storage identified during the SmallFlex project is the upper part of the headrace tunnel. This volume should represent an increase in the storage capacity by 50% and a decrease of the available head by one-third. To investigate the influence of decreasing the head on the Pelton turbine performances, four simulations for a needle stroke of 90% have been carried out corresponding to 100%, 84%, 75% and 66% of the nominal head.

Figure 1: Picture of the Pelton wheel.

3. NUMERICAL SET UP

To reduce the CPU resources required to run a simulation, the computational domain is simplified by considering only half of the runner with only two consecutive jets and six runner buckets (see Figure 2 left) instead of six jets and twenty-one buckets. The fixed and rotating domains are meshed separately with tetrahedrons (see Figure 2 right). Three prism layers are added along the solid walls to improve the computation of the boundary layers. The total number of cells is around 45 million with 26 million of cells in the rotating

domain. The averaged y^+ is lower than 300 excepted close to the nose of the needle. The mesh connectivity at the rotor/stator interface is controlled using the General Grid Interface (GGI) method.

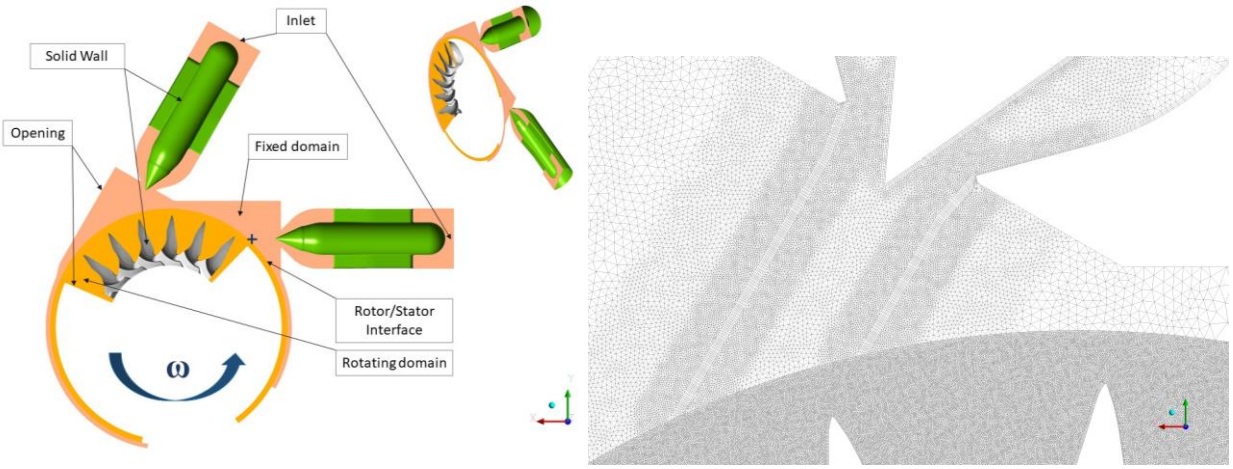

Figure 2: Left: View of the computational domain (the cross refers to the probe position for the jet velocity monitoring). Right: View of the mesh.

The flow is solved using the U-RANS equations written for a homogenous two-phase flow composed of air (at 25°C and 1 atm) and water. Turbulence is modelled with the Boussinesq's assumption that introduces an eddy viscosity computed using the SST k-ω model coupled with an insensitive y^+ wall law. The interface between the two fluids is treated using the free surface option available in Ansys CFX to limit the interface diffusion.
At the inlet of the injectors, the total pressure, calculated from the head, is imposed and the air volume fraction is set to zero. At the opening boundaries, an opening pressure boundary condition is set with a zero gradient conditions for both the air and liquid volume fractions. The solid walls are considered as no-slip walls.
The second order backward Euler scheme is used for the time integration with a time step fixed to 0.4 degree of rotation per time step. This time step corresponds to a RMS CFL number around 3. At each time step, at least 3 internal loops are computed with a maximum of 6 loops. The convective fluxes are discretized using a high order scheme for both the momentum and turbulent conservation equations.
The flow is first initialized without the runner rotation during 0.04 s to allow the development of the jets. Then the rotation of the runner buckets is started and the flow is computed during 0.067 s, which corresponds to a runner rotation angle of 240 degrees.

4. RESULTS

Figure 3 shows the time-history of the dimensionless jet velocity monitored downstream the first nozzle (see Figure 2 left). The jet is well established before the runner rotation starts. Whatever the head, the dimensionless velocity reaches 0.97, which is a typical value of the k_c coefficient of a Pelton turbine [20].

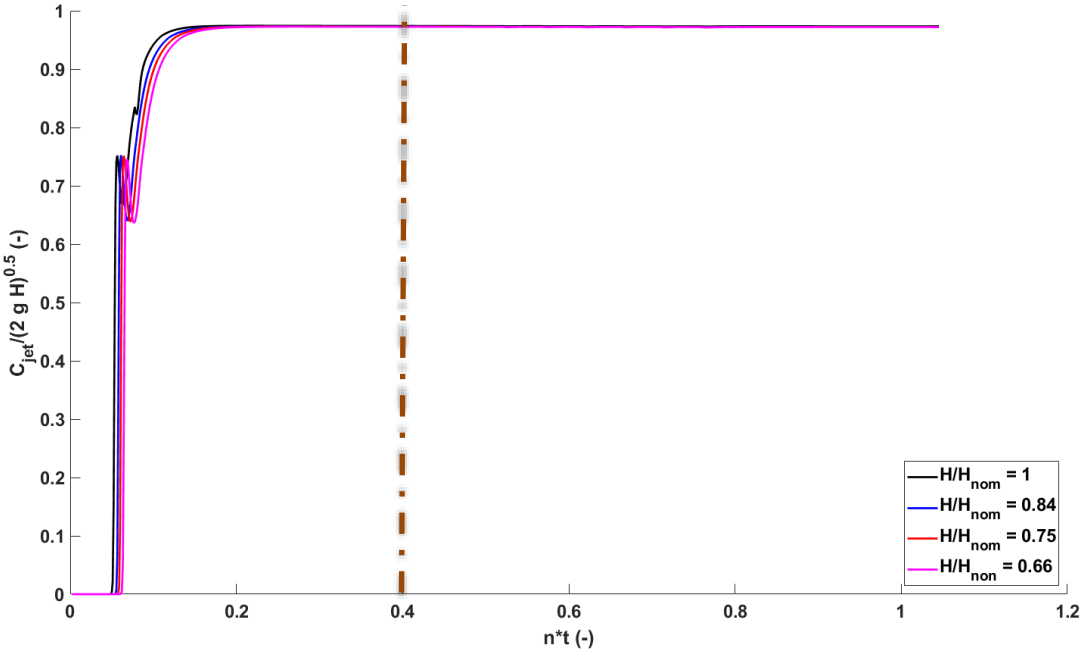

Figure 3: Time-history of the dimensionless jet velocity for each head computed. The dash-dot line refers to the time at which the rotation of the runner buckets starts.

The RMS and maximum RMS of each equation solved is shown in Figure 4 for the simulations at the nominal head and 75% of the nominal head. The RMS never exceed 10^{-3} whereas the maximum RMS are below 1. No peak or increase tendency are observed on the RMS.

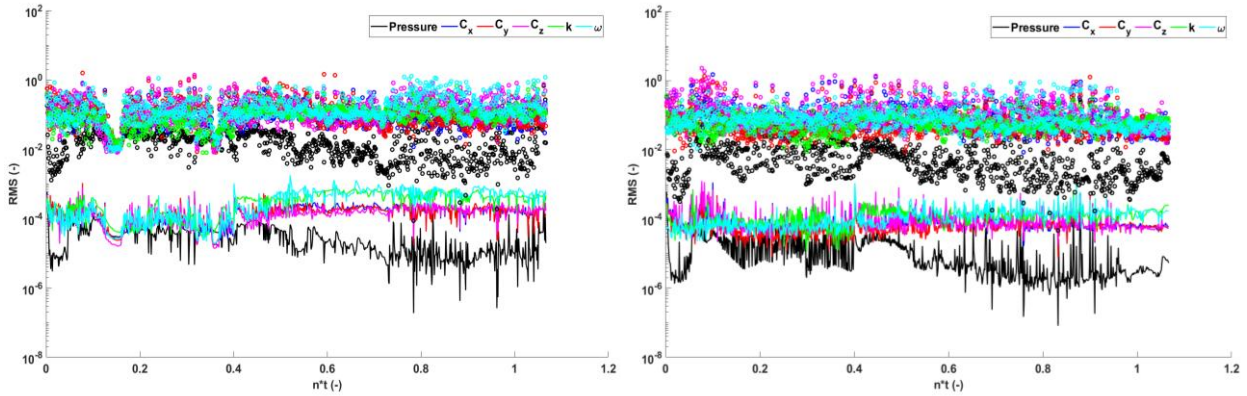

Figure 4: Time-history of the RMS (lines) and maximum RMS (symbols) of each equation solved for the simulations at nominal head (left) and 75% of the nominal head (right)

The on-site measurements allowed determining the relation between the needle stroke and the flow rate for one injector. The simulated flow rates for six opened injectors are then calculated and compared with this relation in Table 1. The simulations underestimate the flow rate by less than 3%.

H/H_{nom} (-)	Q_{CFD}/Q_{nom} (-)	Q_{EXP}/Q_{nom} (-)	Relative error (%)
1	1.17	1.20	-2.0
0.84	1.07	1.09	-1.7
0.75	1.00	1.02	-1.2
0.66	0.95	0.98	-3.0

Table 1: Comparison of the simulated and measured flow rate for each head.

Since only two jets and six buckets are considered in the simulations, a calculation procedure has been developed to reconstruct the runner torque for six jets in operation. First, the torques on each bucket due to two consecutive jets are time shifted and superimposed (see Figure 5). It is noticeable that the torque is identical

for the first five buckets whereas for the last bucket the torque is lower. This is explained by the absence of a seven bucket.

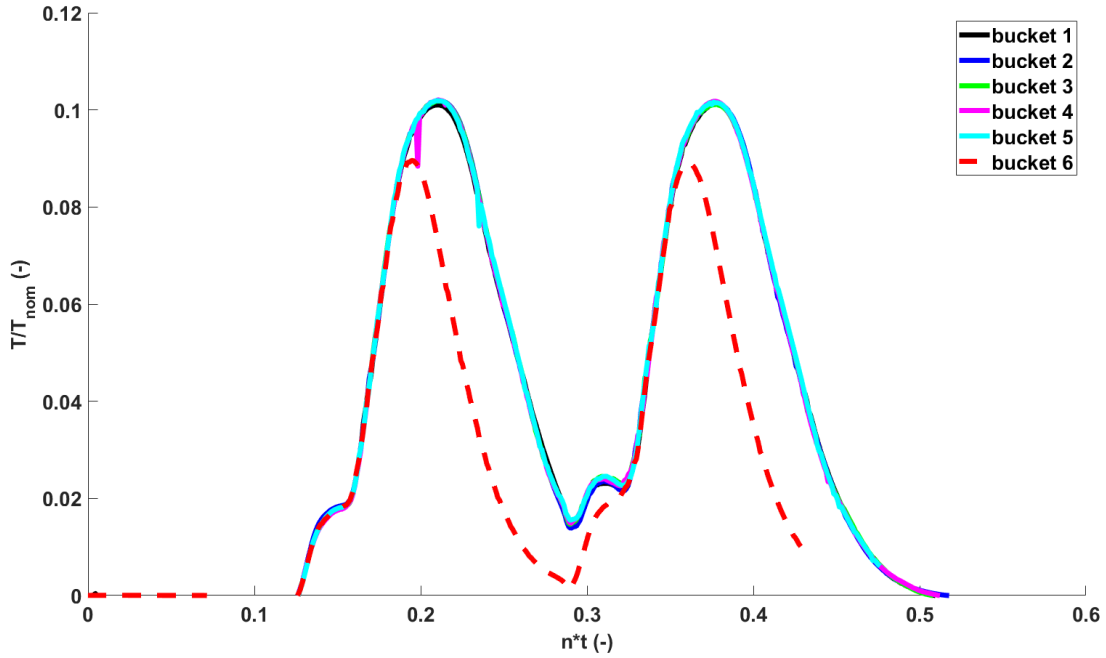

Figure 5: Torque on each bucket due to two consecutive jets. The torques are time shifted and superimposed. Simulation at the nominal head.

Then, for each head, the torque is averaged over the five first buckets (see Figure 6) to get the torque on one bucket impacted by two consecutive jets. By lowering the head, the bump due to the loading of the bucket by the second jet increases due to the interaction between the two consecutive jets.

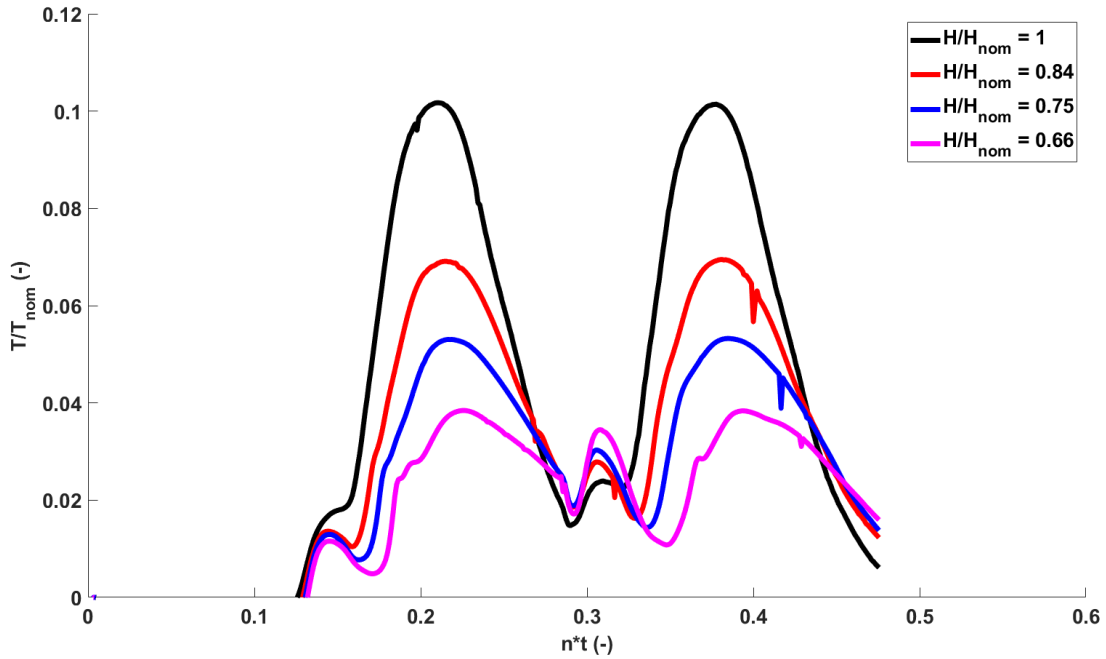

Figure 6: Torque on a single bucket due to two consecutive jets calculated by averaging the torque on the first five buckets.

Finally, only the torque due to the second jet (between n^*t = 0.3 and n^*t = 0.47) is used to reconstruct the runner total torque due to six jets in operation. Figure 7 displays this reconstructed torque from a startup. Oscillations of the torque are observed for each head, they are equal to less than 3% of the average value for the nominal head and increase by lowering the head around 6% for the lowest head.

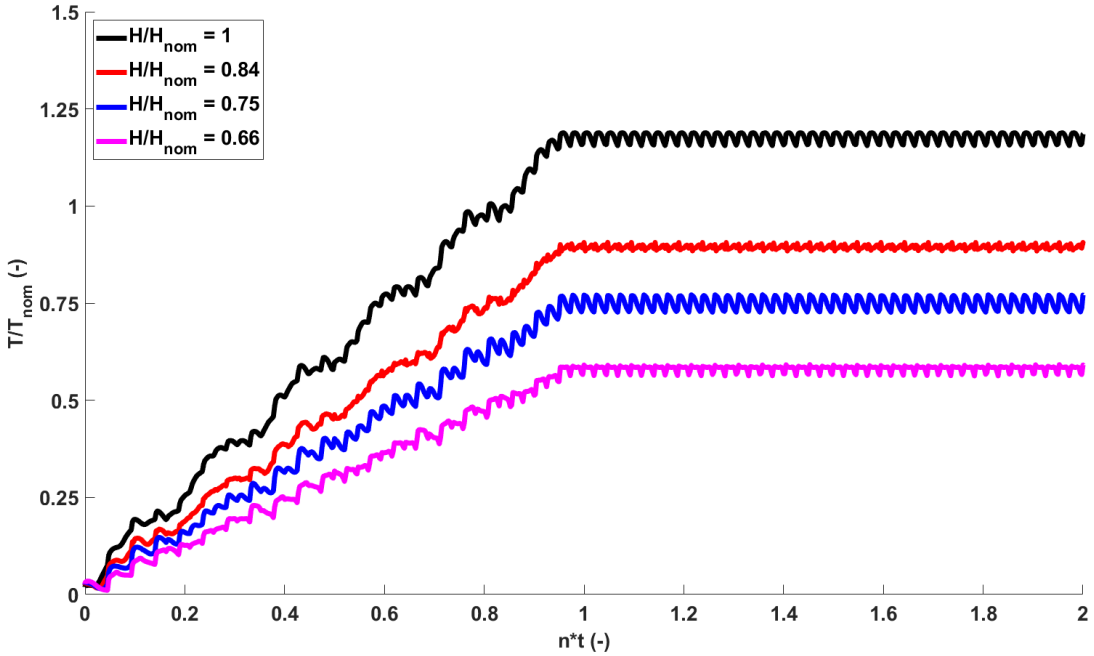

Figure 7: Total runner torque for the Pelton runner with six jets in operation reconstructed from the CFD results.

The average total torque is used to compute the mechanical power that is compared to the measured output power (after the turbine generator unit) in Table 1. The efficiency of the turbine generator is expected to be above 98%. Therefore, the two powers should be close one to each other. At the nominal head, the relative error is lower than 1% between these two powers. At 84% of the nominal, the relative error increases to 9%. For lower heads, the discrepancy still increases and reaches 56% for the lowest head. Consequently, the efficiency is well predicted only for the nominal head. For lowers heads, the drop in efficiency due to the head lowering is underestimated by the simulations with only a small decrease by 8% between the nominal head and the lowest head instead of 41% (see Table 3). The "falaise" effect is therefore not accurately captured by the simulations.

H/H_{nom} (-)	$P_{m,CFD}/P_{m,nom}$ (-)	$P_{out,EXP}/P_{m,nom}$ (-)	Relative error (%)
1	1.18	1.17	0.72
0.84	0.89	0.82	8.87
0.75	0.75	0.54	38.2
0.66	0.58	0.37	56.1

Table 2: Comparison of the simulated and measured power for each head.

H/H_{nom} (-)	η_{CFD} (-)	η_{EXP} (-)	Relative error (%)
1	0.89	0.87	2.85
0.84	0.89	0.80	10.8
0.75	0.88	0.63	39.8
0.66	0.82	0.51	60.9

Table 3: Comparison of the simulated and measured efficiency for each head.

However, the simulations show the interaction between the two consecutive jets and its role on the efficiency drop. Figure 8 compares the dimensionless velocity in the symmetry plane between the simulations at the nominal head and at the lowest head. The bucket 3 starts to be impacted by the second jet. However, due to a lower jet velocity for the case at H/H_{nom} = 0.66, the bucket 3 is not empty when the second jet impacts the

bucket (see the red circle in Figure 9). Therefore, the second jet impact directly on a water sheet, which limits the torque generated.

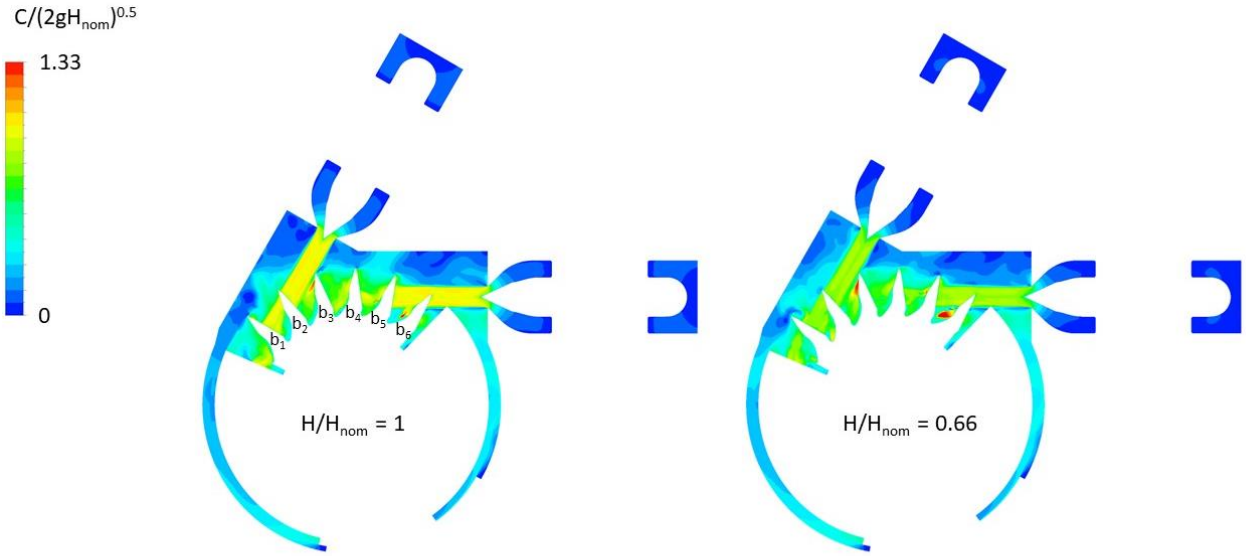

Figure 8: Contours of the dimensionless velocity magnitude in the symmetry plane at t^*n = 0.38 (same time reference than Figure 6).

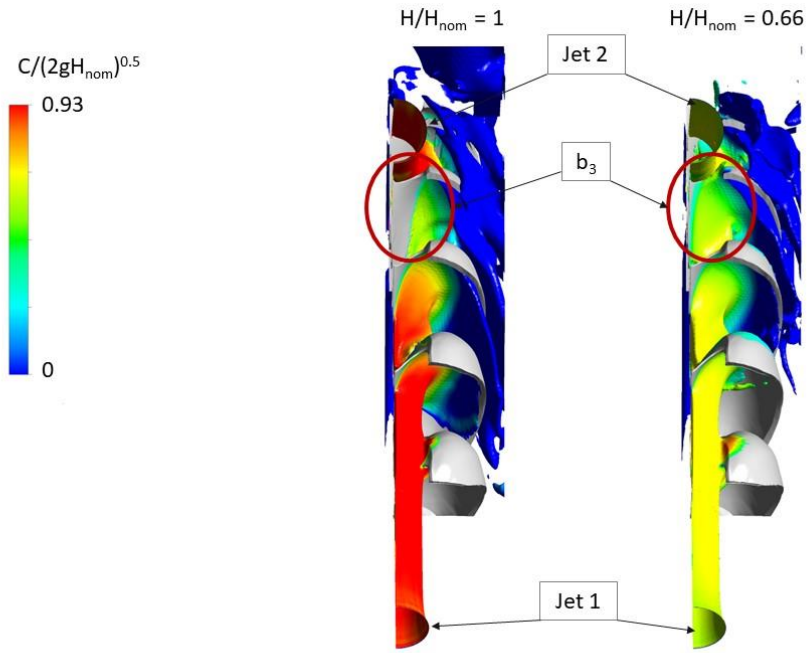

Figure 9: Iso-surface of the water liquid fraction equal to 0.5 colored by the dimensionless velocity at t^*n = 0.38 (same time reference than Figure 6).

Furthermore, the pressure on the leading edge of the bucket decreases by lowering the head (see Figure 10), which can lead to:

- a change in the mechanical stresses responsible for a premature fatigue,
- cavitation inception responsible for local erosion reducing the performance of the bucket.

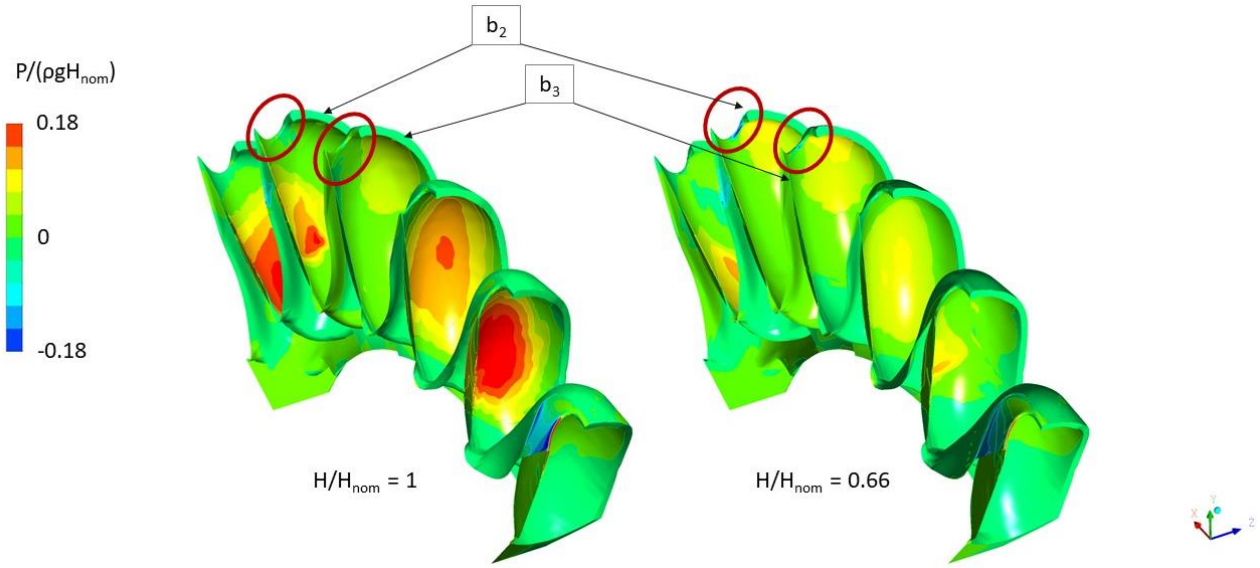

Figure 10: Dimensionless relative pressure on the buckets at t^*n = 0.38 (same time reference than Figure 6).

5. CONCLUSIONS

In the framework of the SmallFlex project, one objective focuses on the use of the upper part of the headrace tunnel as an additional storage volume. The use of this volume requires operating the Pelton turbine at lower heads than the one for which the turbine was designed.

The influence of the head on the interaction between two consecutive jets of the six-jet Pelton turbine has been simulated by CFD using the Ansys CFX software. To reduce the CPU resources, a half of the turbine with only six buckets and two jets has been considered. The lowest head investigated corresponds to 66% of the nominal head, i.e., the emptying of one-third of the headrace tunnel.

The jets are well predicted by the simulations with a relative error of less than 3% on the flow discharge compared to the measurements. The power and the efficiency are also predicted with less than 3% error but only at the nominal head. By lowering the head, the discrepancy between the simulations and the on-site measurements increases to 60%. Consequently, the simulations underestimate the efficiency drop also named "falaise" effect observed experimentally. However, the mechanisms responsible for the efficiency drop can be partially identified by analyzing the CFD results. By lowering the head, the jet velocity decreases, which prevents the water sheet to escape from the bucket before the bucket was impacted by the second jet. The shock between the jet and the water sheet increases the hydraulic losses. In addition, the simulation shows low pressure zones at the lowest head compared to the nominal head, which could provoke cavitation erosion.

To improve the accuracy of the simulations, at least two tracks should be considered: the influence of the size of the computational domain and the influence of the free surface option specified in the set up. The latter prevents the breaking of the water sheets and the development of bubbly flow outside of the bucket as observed experimentally.

NOMENCLATURE

CFD	Computational Fluid Dynamics
CPU	Computational Power Unit
C_{jet}	Jet velocity (m s^{-1})
g	Gravitation acceleration (m s^{-2})
H	Head (m)
k	Turbulent kinetic energy (m^2 s^{-2})
n	Rotational speed (Hz)

P_h	Hydraulic power (W)
P_m	Mechanical power (W)
P_{out}	Output power (W)
Q	Flow discharge (m^3 s^{-1})
RMS	Root Mean Square
SST	Shear Stress Transport
t	time (s)
URANS	Unsteady Reynolds-Averaged Navier-Stokes
ω	rotational speed (rad/s)
ω	turbulent eddy frequency (s^{-1})
nom	subscript for nominal conditions

ACKNOWLEDGEMENTS

The SmallFLEX project has received financial support from SFOE (SI/501636-01) and from FMV. The project was carried out in the framework of the Swiss Competence Center for Energy Research for the Supply of Electricity, SCCER-SoE. The authors would like to thank EAWAG, PVE, WSL and Hydro Exploitation SA for their collaboration and support.

REFERENCE AND CITATIONS

[1] Office fédéral de l'énergie. (2015). Statistique suisse de l'électricité 2015. Berne.

[2] Office fédéral de l'énergie. (2019). Statistique suisse de l'électricité 2019. Berne.

[3] Mohd, A., Ortjohann, E., Schmelter, A., Hamsic, N.; Morton, D., Westphalia, S., Sciences, A., Soest, D. & Ring, L. (2008). Challenges in integrating distributed Energy storage systems into future smart grid. IEEE International Symposium on Industrial Electronics. 1627-1632.

[4] https://www.bfe.admin.ch/bfe/fr/home/approvisionnement/energies-renouvelables/force-hydraulique/petite-hydraulique.html, visited the 17th of March 2021.

[5] Müller, A, Münch-Alligné, C, Nicolet, C, Denis, V, & Avellan, F, (2019). Pushing the envelope: Switzerland's approach to unlocking hidden hydropower potential., Hydro Congress, Porto. Portugal.

[6] Münch-Alligné, C., Decaix, J., Gaspoz, A., Hasmatuchi, V., Dreyer, M., Nicolet, C., Alimirzazadeh, S., Zordan, J., Manso, P., Crettenand, S. (2021). Production flexibility of small run-of-river power plants: KWGO smart-storage case study. 30th Symposium on Hydraulic Machinery and Systems, Lausanne, Switzerland.

[7] Zhang, Z. (2016). *Pelton Turbines*. Springer-Verlag GmbH.

[8] Perrig, A. Valle, M. Farhat, M. Parkinson, E. Favre, J. & Avellan, F. (2006). Onboard flow visualization in a Pelton turbine bucket. 23rd IAHR Symposium.

[9] Thake, J. (2001), *The Micro-Hydro Pelton Turbine Manual: Design, Manufacture and Installation for Small-Scale Hydro-Power*. Paperbackshop UK Import

[10] Jost, D., Meznar, P. & Lipej, A. Numerical prediction of Pelton turbine efficiency IOP Conf. Series: Earth and Environmental Science 12, 012080

[11] Patel, K.; Patel, B.; Yadav, M. & Foggia, T. (2010). Development of Pelton turbine using numerical simulation IOP Conf. Series: Earth and Environmental Science 12, 012048

[12] Pavesi, G., Rossetti, A., Santolin, A. & Ardizzon, G. (2013). Numerical Analyses of a Cavitating Pelton Turbine ETC-13, 1-12

[13] Chongji, Z., Yexiang, X., Zhu, W., Yao, Y. Y. & Wang, Z. (2015). Numerical simulation of cavitation flow characteristic on Pelton turbine bucket surface IOP Conf. Series: Materials Science and Engineering 72

[14] Staubli, T., Abgottspon, A., Weibel, P., Bissel, C., Parkinson, E., Leduc, J. & Leboeuf, F. (2009). Jet quality and Pelton efficiency, Hydro 2009, Lyon, France

[15] Peron, M.; Parkinson, E.; Geppert, L. & Thomas, S. (2008). Importance of the jet quality on the Pelton efficiency and cavitation, International Conference on Hydraulic Efficiency Measurements - IGHEM 2008 - Milano 3rd-6th September, 1-9

[16] Marongiu, J. C., Leboeuf, F. & Parkinson, E. (2007). Numerical simulation of the flow in a Pelton turbine using the meshless method smoothed particle hydrodynamics: a new simple solid boundary treatment, Proc. IMechE Part A: J. Power and Energy, 221, 849-856

[17] Vessaz, C., Andolfatto, L., Avellan, F. & Tournier, C. (2017). Toward design optimization of a Pelton turbine runner, Structural and Multidisciplinary Optimization, 55, 37-51

[18] Leguizamón, S., Alimirzazadeh, S., Jahanbakhsh, E. & Avellan, F. (2020), Multiscale simulation of erosive wear in a prototype-scale Pelton runner, Renewable Energy, Elsevier BV, 151, 204-215

[19] Židonis, A. & Aggidis, G. A. (2015). State of the art in numerical modelling of Pelton turbines. Renewable and Sustainable Energy Reviews. Elsevier BV. 45. 135-144.

[20] Gupta, S. C. (2006). *Fluid Mechanics and Hydraulic Machines*. Pearson India.